H, s); vinyl 6.26 (2 H, m), 6.18 (1 H, m); =CHCH=C(CN)$_2$ 6.84 (1 H, d), 7.67 (1 H, s); meso H 8.26 (1 H, s), 9.86 (2 H, s), 9.89 (1 H, s); NH -3.6 (1 H, s), -4.1 (1 H, s).

Ethyl Cyanoacetate Adduct (4e). This was prepared as in (i) for malononitrile. Reaction required about 10 h for completion. Isosbestic points: 380, 455, 535, 655 nm.

Pyrrolidine Hemiaminal. To $\sim 10^{-5}$ M **1b** in THF or CH_2Cl_2 was added 1 drop of pyrrolidine. Reaction was completed within 30 min. Isosbestic points (THF): 321, ~370, 423, 496, 578, 602, 628 nm.

Schiff Base Protonation/Deprotonation. (i) HF, HCl, HBr in CH_2Cl_2: To $\sim 10^{-5}$ M **1c** or **4c** in CH_2Cl_2 was bubbled air which had been equilibrated over the respective concentrated acid. (This was easily accomplished by withdrawing the air inside a bottle of acid with a small syringe and then passing the air into the cuvette.) The resultant SB·HCl spectra were identical as in (ii). BF_3OEt_2 was introduced to SB·HF by bubbling BF_3OEt_2-saturated air through the solution. (ii) To $\sim 10^{-5}$ M Schiff base in CH_2Cl_2, THF, or CH_3CN was added dropwise an anhydrous HCl-saturated CH_2Cl_2 solution. (iii) HI: To $\sim 10^{-5}$ M **1c** or **4c** in CH_2Cl_2 was injected a small amount of HI vapor prepared by adding concentrated sulfuric acid to KI. (iv) $HClO_4$: To $\sim 10^{-5}$ M Schiff base in CH_2Cl_2, THF, or CH_3CN was added dropwise a 70% $HClO_4$-saturated methylene chloride solution. (v) SBH^+ were returned to the original SB by bubbling triethylamine-saturated air through the acidified solution.

Borohydride Reduction. To $\sim 10^{-5}$ M **4b** in CH_2Cl_2 was added a couple of crystals of tetrabutylammonium borohydride and the UV-vis spectrum monitored. Isosbestic points: 321, 370, 423, 496, 578, 602, 628 nm. Addition of 2 drops of a 1:1:1 CH_3OH:TFA:H_2O solution yielded a typical copper porphyrin spectrum. Isosbestic points: 313, 345, 369, 409, 544, 557, 582 nm, λ_{max} (Cu porphyrin) 400, 528, 570 nm.

Acknowledgment. This work was supported in part by the NSF. We thank Professor G. T. Babcock and Dr. Pat Callahan for kindling our interest in Schiff base porphyrins and Professor G. Maggiora for communicating results prior to publication. C.K.C. is an Alfred P. Sloan Fellow, 1980-1984, and a recipient of a Camille and Henry Dreyfus Teacher-Scholar Grant, 1981-1985.

Registry No. 1a, 86146-16-9; **1b**, 84195-13-1; **1c**, 84195-14-2; **1c**·HF, 90413-37-9; **1c**·HCl, 90413-38-0; **1c**·HBr, 90413-39-1; **1c**·HI, 90413-40-4; **1c**·$HClO_4$, 90413-41-5; **1c**·HBF_4, 90413-42-6; **2a**, 90413-52-8; **2b**, 90413-26-6; **2c**, 90413-27-7; **3a**, 86146-17-0; **3b**, 90413-28-8; **3c**, 90413-29-9; **4a**, 90413-53-9; **4b**, 90413-30-2; **4c**, 90413-31-3; **4c**·HF, 90413-43-7; **4c**·HCl, 90413-44-8; **4c**·HBr, 90413-45-9; **4c**·HI, 90413-46-0; **4c**·$HClO_4$, 90413-47-1; **4c**·HBF_4, 90413-48-2; **4d**, 90413-32-4; **4d**·Cl^-, 90413-49-3; **4d**·Br^-, 90413-50-6; **4d**·ClO_4^-, 90413-51-7; **4e**, 90413-33-5; **4f**, 90413-34-6; **5a**, 90413-54-0; **5b**, 90413-35-7; **5c**, 90413-36-8; **5c**·$(CF_3COOH)_2$, 90432-15-8.

Spectral Properties of Protonated Schiff Base Porphyrins and Chlorins. INDO-CI Calculations and Resonance Raman Studies

Louise Karle Hanson,*[1b] C. K. Chang,*[1a] Brian Ward,[1a] Patricia M. Callahan,[1a,c] Gerald T. Babcock,*[1a] and John D. Head[1b,d]

Contribution from the Department of Chemistry, Michigan State University, East Lansing, Michigan 48824, and the Department of Applied Science, Brookhaven National Laboratory, Upton, New York 11973. *Received October 6, 1983*

Abstract: INDO-CI calculations successfully reproduce the striking changes in optical spectra that occur upon protonation of mono- and disubstituted porphyrin, chlorin, and bacteriochlorin Schiff base complexes. They ascribe the changes to Schiff base C=N π^* orbitals which drop in energy upon protonation and mix with and perturb the π^* orbitals of the macrocycle, a result consistent with resonance Raman data. The perturbation is predicted to affect not only transition energies and intensities but also dipole moment directions. The symmetry of the porphyrin and the substitution site of the chlorin are shown to play an important role, especially in governing whether the lowest energy transition will red shift or blue shift. Blue shifts are calculated for protonation of ketimine and enamine isomers of pyrochlorophyll *a* (PChl). Comparison with reported optical spectra suggests that PChl *a* Schiff base may undergo isomerization upon protonation. Resonance Raman data on CHO, CHNR, $CHNHR^+$, and pyrrolidine adducts of chlorin demonstrate the isolation of the peripheral C=O and C=N groups from the macrocycle π system, intramolecular hydrogen bonding, and selective enhancement of $\nu_{C=N}$ for those species with a split Soret band. $\nu_{C=N}$ is observed with 488.0-nm excitation into the lower-energy Soret and absent for 406.7-nm excitation into the higher-energy Soret, a result predicted by the calculations.

Photosynthesis in algae and green plants functions via two chlorophyll (Chl)-mediated systems which cooperatively reduce carbon dioxide (Photosystem I, PS I) and oxidize water (PS II).[2] Light is absorbed by antenna pigments (mostly Chl) which then funnel the excitation energy to special chlorophylls within the reaction centers, P700 in PS I and P680 in PS II. These pigments function as phototraps by virtue of their red-shifted absorption spectra relative to the antenna Chl. P700 and P680 are the primary electron donors for the light-driven reactions; the electron transfer takes place from their first excited singlet states.

Monomeric Chl *a* absorbs at 663 nm in CH_2Cl_2/THF[3] and P680 and P700 at 680 and 700 nm, respectively. The redox potentials of P700 and P680 are also modulated, P700 is ~0.3-0.4 V easier and P680 is ~0.1-0.2 V more difficult to oxidize than Chl *a* in CH_2Cl_2.[4] The red-shifted absorption spectra have, until recently, been attributed to dimers or higher-order aggregates of Chl *a*.[4] Because of inconsistencies between spectroscopic data for P680[4] and P700[5,6] and dimeric models, interest has currently

(1) (a) Michigan State University. (b) Brookhaven National Laboratory. (c) Current address: Department of Biochemistry, Molecular and Cell Biology, Northwestern University, Evanston, Illinois 60201. (d) Current address: Quantum Theory Project, University of Florida, Gainesville, Florida 32611.

(2) For recent general surveys of photosynthesis see: Barber, J., Ed. "Primary Processes of Photosynthesis," Elsevier: Amsterdam, 1977. Clayton, R. K. "Photosynthesis: Physical Mechanisms and Chemical Patterns," Cambridge University Press: New York, 1980. "Photosynthesis"; Govindjee, Ed.; Academic Press: New York, 1982; Vol. 1.

(3) Fajer, J.; Fujita, I.; Davis, M. S.; Forman, A.; Hanson, L. K.; Smith, K. M. *Adv. Chem. Ser.* **1982**, *No. 201*, 489-514.

(4) Davis, M. S.; Forman, A.; Fajer, J. *Proc. Natl. Acad. Sci. U.S.A.* **1979**, *76*, 4170-4.

(5) (a) Wasielewski, M. R.; Norris, J. R.; Crespi, H. L.; Harper, J. *J. Am. Chem. Soc.* **1981**, *103*, 7664-5. (b) Wasielewski, M. R.; Norris, J. R.; Shipman, L. L.; Lin, C. P.; Svec, W. A. *Proc. Natl. Acad. Sci. U.S.A.* **1981**, *78*, 2957-61.

0002-7863/84/1506-3950$01.50/0

reverted to monomeric Chl *a*[3-9] whose spectral and redox properties have been altered by the protein environment. Suggestions include ligation to the Chl Mg,[3,4] point charges at the Chl periphery,[7] and derivatization of the carbonyl group on ring V to either an enol[5b] or a Schiff base.[8,9] Schiff base derivatives of pyrochlorophylls have been synthesized which exhibit red shifts of 23–26 nm upon protonation.[8,9]

Several of the present authors have demonstrated[10,11] that the (reversible) modification of carbonyl substituents of metalloporphyrins (P), chlorins (C), and bacteriochlorins (BC) to protonated Schiff base, iminium, ester, and nitrile derivatives can lead to dramatic red shifts of the long wavelength absorption bands, accompanied by splitting or broadening of the Soret band. These spectral perturbations were shown to be modulated by counterion and solvent, and in the case of disubstituted porphyrins they depended upon the substitution symmetry.[11] It is important to understand the origin of these phenomena in order to evaluate the relevance of these derivatives as possible models for reaction center chlorophylls.

Resonance Raman data presented here and previously[10] show that the ground states of the macrocycles remain essentially unperturbed and that the charges of the protonated Schiff base and iminium derivatives are localized on the substituent. We also present theoretical calculations for Schiff base (SB) and protonated Schiff base (SBH^+) mono- and disubstituted porphyrins **1–3**, chlorin **4**, and bacteriochlorin **5**,[12] as well as the ketimine and enamine SB and SBH^+ isomers of pyrochlorophyll *a* (PChl), using a spectroscopic INDO method. Protonation of the Schiff base substituents is shown to perturb the excited states of **1–5** in ways which account for the effects of substitution symmetry, ring reduction, and environment. The calculations duplicate the optical spectra and are consistent with the resonance Raman results.

Methods

INDO-CI Calculations. The theoretical calculations were performed by a spectroscopic INDO method developed by Zerner and co-workers.[13] The method handles transition-metal complexes and includes extensive configuration interaction (CI) for the calculation of optical spectra. We used the program in the INDO/1 mode, with empirical evaluation of the two-center repulsion integrals.[13] The spectra were computed by using 121 single excitations, from the 11 highest-occupied orbitals into the 11 lowest virtual orbitals. The CI portion of the program requires a closed-shell system, hence Ni but not Cu complexes could be calculated. This method has been quite successful in predicting the optical spectra of low-spin ferrous heme complexes.[14]

The formyl Schiff base and protonated Schiff base Ni complexes of **1–5** and the ketimine and enamine Schiff base forms of pyrochlorophyllide *a* were calculated. The coordinates used for **1** and **3** were taken from the crystal structure of **3a**.[15] "Standard" macrocycle coordinates were used for **2**,[16] **4**,[17] and **5**[17] with Ni–N = 2.00 Å. Formyl and Schiff base groups were angled 5° out of plane for **1–3**[15] and coplanar for **4** and **5**. Vinyl substituents were oriented 31° out of plane.[18] **3** and **5** have a center of symmetry (C_i) whereas **2** has either a two-fold axis (C_2) or a mirror plane (C_s). Coordinates for the pyrochlorophyllide *a* Schiff base complexes were taken from the crystal structure of ethyl

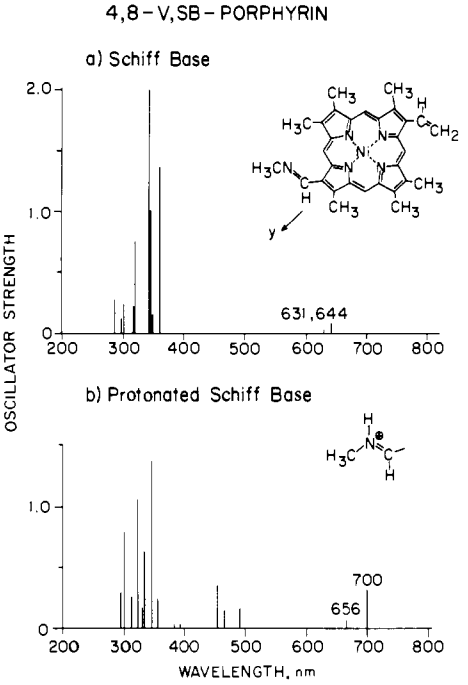

Figure 1. Calculated spectra (oscillator strength vs. λ) of (a) SB **1** and (b) SBH^+ **1**, 4-vinyl, 8-Schiff base porphyrins. The models used in the calculations along with the *y*-axis orientation are given here and on subsequent figures. These spectra have not been corrected by a scaling function. The Q bands tend to fall to the red and the Soret bands to the blue of the actual experimental values. The Q_y bands are the 644- and 700-nm transitions, respectively.

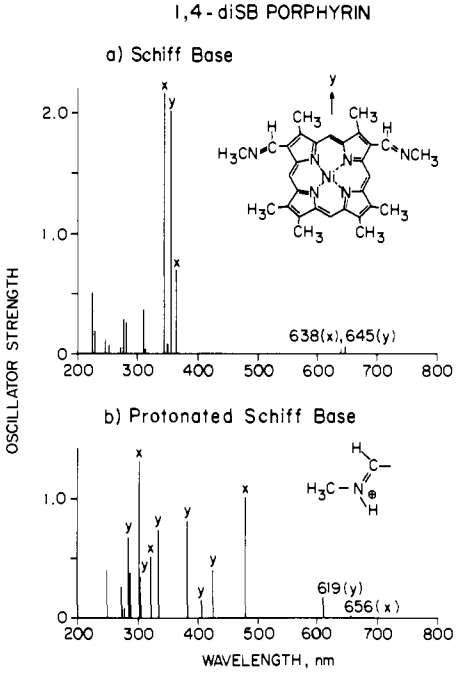

Figure 2. Calculated spectra (oscillator strength vs. λ) of (a) diSB **2** and (b) $diSBH^+$ **2**, 1,4-disubstituted porphyrins. The symmetry element for the complex, either C_2 or *m*, lies along the *y* axis. Spectra were calculated for both symmetries and found to agree within several nm. Shown are the results of the C_2 calculations. The *x* and *y* labels on the transitions indicate their polarizations.

(6) O'Malley, P. J.; Babcock, G. T. *Proc. Natl. Acad. Sci. U.S.A.*, **1984**, *81*, 1098–1111.
(7) (a) Davis, R. C.; Ditson, S. L.; Fentiman, A. F.; Pearlstein, R. M. *J. Am. Chem. Soc.* **1981**, *103*, 6823–6. (b) Eccles, J.; Honig, B. *Proc. Natl. Acad. Sci. U.S.A.* **1983**, *80*, 4959–62.
(8) Pearlstein, R. M.; Ditson, S. L.; Davis, R. C.; Fentiman, A. F.; *Biophys. J.* **1982**, *37*, 112a.
(9) Maggiora, L. L.; Maggiora, G. M. *Photochem. Photobiol.*, in press.
(10) Ward, B.; Callahan, P. M.; Young, R.; Babcock, G. T.; Chang, C. K. *J. Am. Chem. Soc.* **1983**, *105*, 634–6.
(11) Ward, B.; Chang, C. K.; Young, R. *J. Am. Chem. Soc.*, preceding paper.
(12) The numbering refers to Figure 1 of the preceding paper. The exact models used in calculating **1–5** are shown on Figures 1–5.
(13) (a) Ridley, J. E.; Zerner, M. C. *Theor. Chim. Acta* **1973**, *32*, 111–134. (b) Ridley, J. E.; Zerner, M. C. *Ibid.* **1976**, *42*, 223–36. (c) Bacon, A. D.; Zerner, M. C. *Ibid.* **1979**, *53*, 21–54.
(14) (a) Loew, G. H.; Rohmer, M. M. *J. Am. Chem. Soc.* **1980**, *102*, 3655–7. (b) Loew, G., Goldblum, A. *Ibid.* **1980**, *102*, 3657–9. (c) Loew, G. H.; Herman, Z. S.; Zerner, M. C. *Int. J. Quantum Chem.* **1980**, *18*, 481–92.
(15) Chang, C. K.; Hatada, M.; Tulinsky, A. *J. Chem. Soc., Perkin Trans. 2* **1983**, 371–8.
(16) Eaton, W. A.; Hanson, L. K.; Stephens, P. J.; Sutherland, J. C.; Dunn, J. B. R. *J. Am. Chem. Soc.* **1978**, *100*, 4991–5003.
(17) Richardson, P. F.; Chang, C. K.; Hanson, L. K.; Spaulding, L. D.; Fajer, J. *J. Phys. Chem.* **1979**, *83*, 3420–4.
(18) Chow, H.-C.; Serlin, R.; Strouse, C. E. *J. Am. Chem. Soc.* **1975**, *97*, 7230–7.

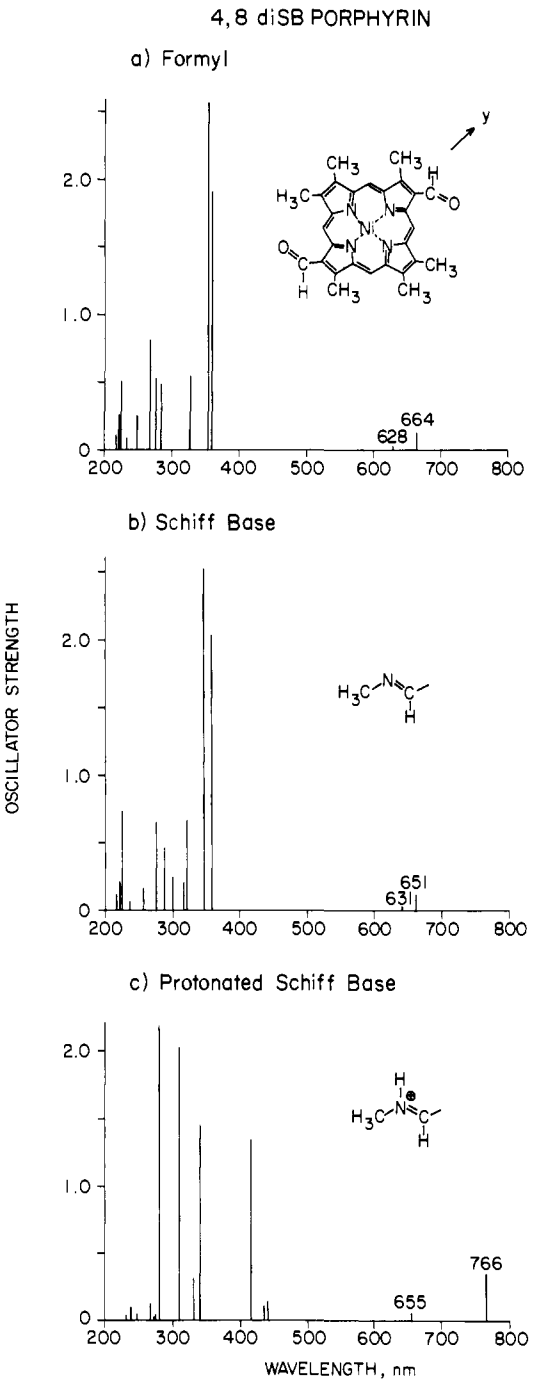

Figure 3. Calculated spectra (oscillator strength vs. λ) of (a) diformyl **3**, (b) diSB **3**, and (c) diSBH$^+$ **3**, 4,8-disubstituted porphyrins. The Q_y bands are the 664-, 651-, and 766-nm transitions, respectively.

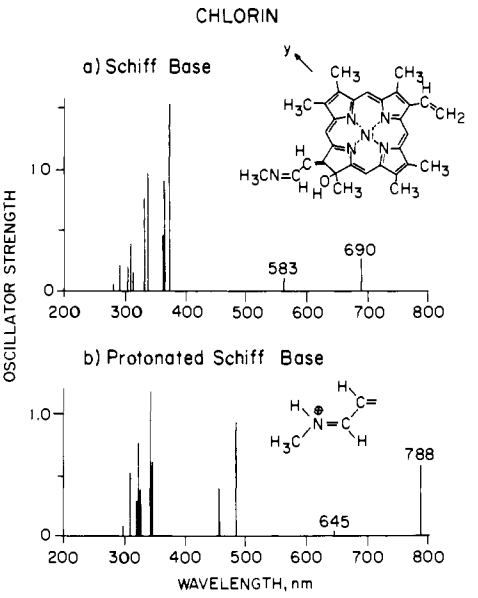

Figure 4. Calculated spectra (oscillator strength vs. λ) of (a) SB **4** and (b) SBH$^+$ **4**, 4-vinyl, 8-Schiff base chlorins. The Q_y bands are the 690- and 788-nm transitions, respectively.

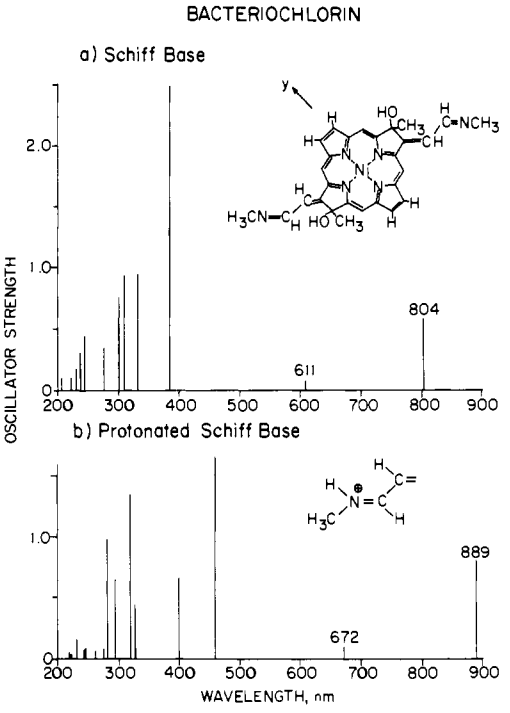

Figure 5. Calculated spectra (oscillator strength vs. λ) of (a) diSB **5** and (b) diSBH$^+$ **5**, 4,8-disubstituted bacteriochlorins. The Q_y bands are the 804- and 889-nm transitions, respectively.

chlorophyllide *a*,[18] with alterations made to ring V in the enamine form to accommodate the double bond. The exact models used for all the calculations are shown on Figures 1–5 and 10.

Resonance Raman Spectroscopy. Resonance Raman (RR) spectra were recorded with a Spex 1401 double monochromator and the associated Ramalog electronics. Laser excitations at 406.7 and 488.0 nm were obtained with a Spectra Physics 164-11 krypton ion laser equipped with a high-field magnet and a Spectra Physics 165 argon ion laser, respectively. Incident powers were 20–40 mW. All spectra were collected at 90° scattering geometry at room temperature. Optical spectra were recorded before and after each RR experiment on a Cary 219 spectrophotometer to ensure that the samples had not decomposed.

Results and Discussion

Calculations on Porphyrins, Chlorin, and Bacteriochlorin. Figures 1–5 present the calculated spectra for mono- and disubstituted Schiff base porphyrins **1–3**, chlorin **4**, and bacteriochlorin **5**. Protonation of the Schiff base substituents of these compounds has been shown[10,11] to induce dramatic changes in the optical spectra (Table I). The Q_y bands[19] red shift and increase in integrated intensity. The Soret band either splits **1–4** or broadens **5**, and in the case of the porphyrins, it loses significant intensity. The calculations duplicate successfully all the major features of the experimental spectra, with the exception of the red shift of **2** (see below). The calculated shifts of Q_y are 1240 cm^{-1} to the

(19) In a metalloporphyrin with fourfold symmetry, the Q_x and Q_y transitions which compose the visible bands are degenerate. The calculations indicate a slight splitting of Q_x and Q_y with the substitution of the formyl and SB groups, the Q_y becoming the more intense and occurring at lower energy. The formyl derivative of **1**, which is analogous to heme *a*, has a calculated splitting of 440 cm^{-1}. Such a splitting has not been detected in the resonance Raman excitation profiles of the Q bands of heme *a* (M. R. Ondrias and G. T. Babcock, unpublished results). However, Choi, et al.[35b] argue from optical spectra that Q_x and Q_y of heme *a* are split by ~1600 cm^{-1}.

Table I. Absorption Maxima for CHO, SB, and SBH^+ Derivatives of **1–5**

compound[a]	solvent	λ_{max}, nm vis	Soret
CHO **1b**	CH_2Cl_2	589	409
SB **1c**		577	404
SBH^+ **1c**·ClO_4^-		635	440, 378
diCHO **2b**	CH_2Cl_2	578	423
diSB **2c**		569	410
SB, SBH^+ **2c**·ClO_4^-		622	452, 423, 382
diSBH^+ **2c**·$(ClO_4^-)_2$		613	456, 388, 339
diCHO **3b**	CH_2Cl_2	606	412
diSB **3c**		584	407
SB,SBH^+ **3c**·ClO_4^-		642	437, 384
diSBH^+ **3c**·$(ClO_4^-)_2$		666	407, 336
CHO **4b**	THF	640	435–394 (br)
SB **4c**		628	425
SBH^+ **4c**·ClO_4^-		735 (br)	490, 404
diCHO **5b**	THF	760	462–403 (br)
diSB **5c**		755	447–402 (br)
diSBH^+ **5c**·$(CF_3CO_2^-)_2$		858 (v br)	501–401 (v br)

[a] The numbering refers to Figure 1 of the preceding paper. The compounds are as follows: (**1b**) nickel(II) 2,6-di-*n*-pentyl-*4-vinyl-8-formyl*-1,3,5,7-tetramethylporphine; (**2b**) nickel(II) 6,7-di-*n*-pentyl-*1,4-diformyl*-2,3,5,8-tetramethylporphine; (**3b**) nickel(II) 2,6-di-*n*-pentyl-*4,8-diformyl*-1,3,5,7-tetramethylporphine; (**4b**) copper(II) 2,6-di-*n*-pentyl-*4-vinyl*-7-hydroxy-*8-acroleinyl*-1,3,5,7-tetramethylchlorin; (**5b**) copper(II) 2,6-di-*n*-pentyl-3,7-dihydroxy-*4,8-diacroleinyl*-1,3,5,7-tetramethylbacteriochlorin.

red, 650 cm^{-1} to the blue, and 2300 cm^{-1} to the red for porphyrins **1–3** and 1800 and 1190 cm^{-1} to the red for the chlorin **4** and bacteriochlorin **5**. Experimental red shifts for the corresponding Ni porphyrin complexes in CH_2Cl_2 with ClO_4^- counterions are 1580, 1260, and 2110 cm^{-1}. Cu chlorin·$HClO_4$ and Cu bacteriochlorin·CF_3CO_2H in THF red shift 2320 and 1590 cm^{-1}, respectively.[20]

Only small differences are observed and predicted between the unprotonated Schiff base (SB) derivatives and their parent aldehydes. The orbital energies (shown for **1**, Figure 6) and calculated spectra (shown for **3**, Figure 3) are very similar. Neither the C=O nor the C=N groups contribute significantly to the highest filled (HOMO) and lowest unoccupied (LUMO) macrocycle orbitals. These results are corroborated by resonance Raman data which indicate that the ground-state structure of the macrocycle is virtually unaffected by exchanging these groups. As can be seen in Figure 8, the aldehyde and SB chlorin derivatives exhibit essentially identical spectra below 1600 cm^{-1}. This will be discussed in more detail later.

In agreement with resonance Raman and NMR results,[10] the calculations also show that protonation of the SB has little effect upon the electronic structure of the ground state. As demonstrated by **1** in Figure 6, the positive charge(s) on the SBH^+ group(s) lowers all the orbital energies, as would any nearby positive charge. Hence the SBH^+ complexes ought to be more difficult to oxidize and easier to reduce. However, there is little direct contribution of the Schiff base C=N atomic orbital coefficients to the macrocycle HOMO π orbitals.

The optical changes are due to excited-state perturbations. Protonation lowers the energy of π^* orbitals localized on the C=N of the Schiff base proportionally more than that of the macrocycle π^* orbitals. For the porphyrins, this results in substantial mixing between the SBπ^* and either one (**1**, **3**) or both (**2**) of the $e_g(\pi^*)$ orbitals, depending on the symmetry of the complex. The LUMO π^* of the reduced porphyrins, **4** and **5**, also mixes with SBπ^* in an identical fashion. As shown in Figure 6, three low-lying π^* orbitals result: the mixed (and lowered) π^*, the unaffected π^*,

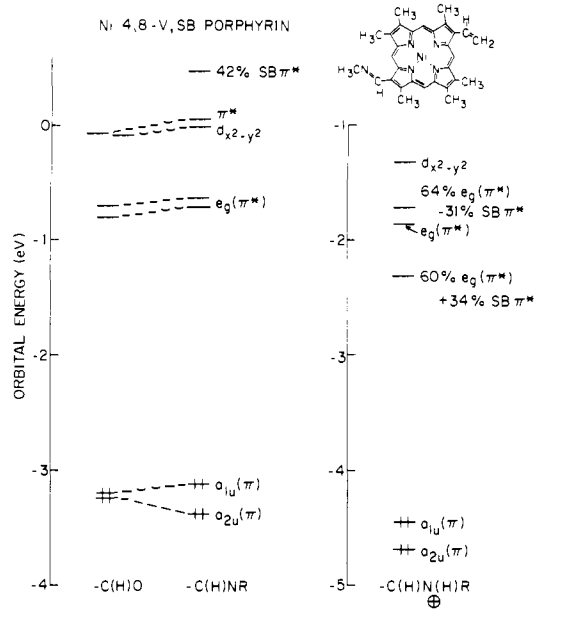

Figure 6. Calculated orbital energy levels for the formyl, SB, and SBH^+ derivatives of **1**. SBπ^* denotes the π^* contribution from the substituent C=N and was determined by summing the squares of the N and C p_z atomic orbital coefficients (the AO coefficients to a given MO are normalized). Note the relative lowering of the SBπ^* orbital and its subsequent mixing with one of the porphyrin $e_g(\pi^*)$ orbitals upon protonation of the Schiff base. The HOMO-LUMO gap is smaller for SBH^+ **1** than for SB **1**. SBH^+ **1** should be more difficult to oxidize, as indicated by its more negative energies; however, the calculations appear to greatly exaggerate the overall drop in potential.

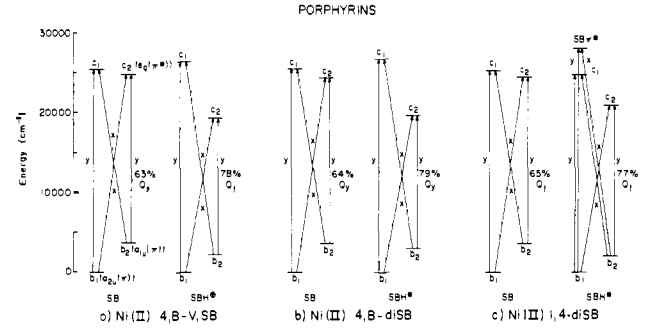

Figure 7. Plot of the relative energies of the highest filled and lowest empty molecular orbitals of the SB and SBH^+ derivatives of the porphyrins (a) **1**, (b) **3**, and (c) **2**, showing the one-electron promotions which constitute the Q_x and Q_y transitions. Q_x consists of the *x*-polarized diagonal promotions and Q_y of the *y*-polarized vertical promotions. The percent contribution of the $b_2 \rightarrow c_2$ promotion to the Q_y is given for each species. "*x*" and "*y*" are not necessarily perpendicular, especially for SBH^+ **1** and **3**: see text. The four-orbital-model nomenclature[23] is used for the porphyrin a_{1u}, $a_{2u}(\pi)$, and $e_g(\pi^*)$ orbitals. The orbitals for each species have been plotted relative to b_1 set at zero.

and a second, slightly higher energy SBπ^*,π^* hybrid. Essentially the same results are obtained with charge-iterative extended Hückel calculations[21] and molecular fragment ab initio calculations[22] for **1**. Plots of electrochemical redox potentials for malononitrile and ethyl cyanonitrile adducts of **4**,[11] species which exhibit SBH^+-like optical spectra, give similar orbital patterns.

The environment of the SBH^+ group—solvent and counterion—has been shown to affect the optical spectra of the protonated species.[11] In general, the largest spectral perturbations are observed under conditions which result in greater localization of the charge on the SBH^+ group. These observations agree well

(20) The calculations were performed on the bare protonated species with no counterion present. The red shifts manifested by the experimental spectra were found to depend on solvent and counterion.[11] The values given for **1–3** represent conditions for observing the maximum shifts. The values given for **4** and **5** are internally consistent (**5** was not measured in CH_2Cl_2).

(21) L. K. Hanson and B. Foy, unpublished results.

(22) Petke, J. D.; Maggiora, G. M. *J. Am. Chem. Soc.*, In press. Their calculated spectra for SB and SBH^+ **1** also nicely duplicate the major changes induced by protonation.

with the mixing mechanism suggested by the calculations: the larger the effective charge on the C=N, the more the SBπ^* orbital will be lowered, the greater the mixing with the macrocycle π^*, and the larger the subsequent perturbation to the optical spectrum.

Many features of the optical spectra of porphyrins can be rationalized in terms of the "four orbital" model of Gouterman,[23] wherein the visible (Q) and Soret (B) bands are due to (−, +) combinations of one-electron promotions between the two highest occupied π orbitals b_1 (a_{2u}) and b_2 (a_{1u}) and the two lowest unoccupied π^* orbitals c_1, c_2 (e_{gx}, e_{gy}). Q_y arises from the two y-polarized promotions ($b_2 \rightarrow c_2$) − ($b_1 \rightarrow c_1$) and Q_x from the two x-polarized promotions ($b_1 \rightarrow c_2$) − ($b_2 \rightarrow c_1$) (see Figure 7). If the b_1, b_2 and c_1, c_2 orbitals are degenerate in energy, the two promotions, say for y, contribute equally to Q_y and effectively cancel each other. However, the more skewed the orbital energies, the more the lower energy promotion contributes to Q_y. Q_y then shifts to lower energy and increases in oscillator strength.

The calculations correctly predict the relative red shifts of Q_y as **3** > **1** and **4** > **5**. In Figure 7 are plotted the orbitals that give rise to the Q_y bands for the SB and SBH$^+$ derivatives of **1**–**3**. **1** and **3** conform to the "classical" picture. For the SBH$^+$ derivatives, the introduction of substantial Schiff base π^* character into one of the $e_g(\pi^*)$ orbitals, c_2, significantly lowers that orbital. The Q_y bands, now composed of a larger percentage of the lower-energy $b_2 \rightarrow c_2$ promotion, are thereby red shifted and more intense, the diSBH$^+$ **3** more so than the monoSBH$^+$ **1**. For reduced porphyrins, the two lowest empty π^* orbitals are never degenerate, with bacteriochlorin split more than chlorin.[23,24] Thus, widening the gap between c_1 and c_2 by lowering c_2 affects **5** less than **4**. The increase in the percent contribution of the $b_2 \rightarrow c_2$ promotion to Q_y upon protonation is smaller for **5** (86% to 87.5% as compared to 78% to 82% for **4**), resulting in less of a red shift.

Experimentally, Q of diSBH$^+$ **2** is red shifted less than that of the monoSBH$^+$ **1** (1260 vs. 1580 cm^{-1}). Indeed, the titration data[11] reveal that addition of one proton to **2** red shifts Q by 1500 cm^{-1} and that addition of the second proton slightly blue shifts Q by 240 cm^{-1}. Figure 7 shows that the situation for diSBH$^+$ **2** is complicated by an additional low-lying Schiff base π^* orbital. Q_y arises from *three* promotions, not two. The contribution of the $b_2 \rightarrow c_2$ is still enhanced, increasing the Q_y intensity. However, the third promotion, $b_2 \rightarrow$ SBπ^*, which occurs at a higher energy than the porphyrin $\pi \rightarrow \pi^*$, has the net effect of blue shifting the Q_y relative to the unprotonated species. Since the experimental data do reveal a blue shift of the di- vs. the monoprotonated species, it appears that the calculations are basically correct but that they overemphasize the contribution of the third promotion to the Q_y band. A very weak Q_x is calculated with a slight red shift (Figure 2).

An extremely low-lying SBπ^* orbital is also calculated for **SBH$^+$ 1** (Figure 6) and **3**–**5**, but promotions into this orbital do not affect the Q bands due to symmetry considerations. b_1,b_2-(a_{2u},a_{1u}) $\rightarrow$ SBπ^* promotions are strictly forbidden for **3** and **5** because of their C_i symmetry and are accidentally forbidden for **1** and **4**. **1** and **4** have no symmetry so that theoretically any promotion can have any orientation in x, y (and z). It so happens that b_1,$b_2 \rightarrow$ SBπ^* are not coparallel with either b_1,$b_2 \rightarrow c_1$,c_2(Q_y) or b_1,$b_2 \rightarrow c_2$,c_1(Q_x), thus their contribution to the Q bands is negligible. For **2**, however, all promotions are polarized along either x or y so that mixing of b_1,$b_2 \rightarrow$ SBπ^* into the Q transitions is strongly allowed.

The four-orbital model predicts the Soret (B) transitions to be intense because they result from positive combinations of the one-electron promotions: B_y, ($b_1 \rightarrow c_1$) + ($b_2 \rightarrow c_2$), and B_x, ($b_1 \rightarrow c_2$) + ($c_2 \rightarrow b_1$). The more equal in energy the individual promotions, the more intense the transition. Insepection of Figure 7 suggests, therefore, that the splitting of the Soret and its significant loss of oscillator strength for the porphyrin SBH$^+$ derivatives can be rationalized by the dramatic lowering of one $e_g(\pi^*)$ orbital. The intensity of both transitions diminishes because of the inequality of the one-electron promotions. However, SBH$^+$ **4** and **5** experience no net loss in Soret intensity because the SBπ^* perturbation shifts orbitals which were initially quite unequal in energy, **5** more than **4**. The Soret of SBH$^+$ **5** should be and is the least broadened.

The Soret regions predicted by the calculations present a more complicated picture, in that more than two intense transitions may be present, as in SB **1**–**2**, **4**–**5**, and all the SBH$^+$ derivatives.[25] These arise from inclusion of higher energy promotions (into orbitals not shown in Figure 6). Nonetheless, the Soret transitions of the SBH$^+$ derivatives are either split into two distinct regions or broadened. They contain more Schiff base C=N character than the Soret of the unprotonated SB complexes, due not only to the increase of SBπ^* in the LUMO π^* orbitals but also to higher-energy promotions into other orbitals with a substantial SBπ^* contribution. The distribution of this C=N character is not always uniform throughout the Soret region. The lower-energy branch of the Soret (Soret 1) is predicted to have more SB C=N π^* character than the higher-energy branch (Soret 2) for SBH$^+$ **1** and **4**, with the greatest differential predicted for **4**. Resonance Raman studies tend to confirm this prediction. For **4**, excitation into Soret 1 yielded enhancement of the peripheral C=N stretch, whereas this band was absent with excitation into the maximum of Soret 2. For **1**, C=N enhancement was observed for excitation into Soret 1[11] and the short wavelength side of Soret 2.[26] Transitions which contain more C=N character should be more sensitive to the degree of SBπ^*, macrocycle mixing. Indeed, environmental factors such as solvent and counterion were found to affect the lower- but not the higher-energy branch of the Soret of SBH$^+$ **1** and **4**.[11]

The mixing of SBπ^* with the macrocycle π^* orbitals is predicted to affect not only transition energies and intensities but also the dipole moment directions of **1** and **3**–**5**, complexes with no fixed symmetry axes. (For **2**, y-polarized transitions lie along the symmetry element, either m or C_2, which runs along the methine carbon axis between the two substituted pyrrole rings (Figure 2). The x-polarized transitions are perpendicular to y.) Table II gives the polarization data for **1** and **3**–**5**. For porphyrins **1** and **3**, some of the predicted changes are quite dramatic. Q_y lies within 21° of the pyrrole nitrogens of the substituted pyrrole rings. It is approximately perpendicular to Q_x only in the SB derivatives. Surprisingly, Q_y and Q_x are predicted to be 26.5° apart in SBH$^+$ **1**[27] and 67.5° apart in SBH$^+$ **3**. Although the Soret transitions are more complicated (see above), B_y and B_x can be assigned to the most intense transitions of SB **1** and **3**. The transition dipoles of SBH$^+$ **1** and **3** point every which way, however, with no obvious similarity to each other or to **2**. MCD, a spectroscopic technique sensitive to the relative orientation of transition dipoles,[28] may provide a way of testing the calculations. Each protonated Schiff base porphyrin is predicted to exhibit a different MCD spectrum in both the visible and the Soret bands.

For the SB derivatives of the reduced porphyrins, **4** and **5**, Q_y lies within 17° of the axis through the nitrogens of the unsaturated pyrrole rings (see Figures 4 and 5).[29] Q_y and Q_x are not ap-

(23) (a) Gouterman, M. *J. Mol. Spectrosc.* **1961**, *6*, 138–63. (b) Gouterman, M. In "The Porphyrins"; Dolphin, D., Ed.; Academic Press: New York, 1978; Vol. 3, pp 1–165.

(24) Chang, C. K.; Hanson, L. K.; Richardson, P. F.; Young, R.; Fajer, J. *Proc. Natl. Acad. Sci. U.S.A.* **1981**, *78*, 2652–6.

(25) Molecular fragment ab initio calculations also tend to predict multiple transitions in the Soret region which do not conform to the four-orbital model. For instance, the main contributors to the Soret of Mg chlorin are four intense $\pi \rightarrow \pi^*$ transitions of complex configurational composition. (Petke, J. D.; Maggiora, G. M.; Shipman, L. L.; Christoffersen, R. E. *J. Mol. Spectrosc.* **1978**, *73*, 311–331). We calculate four such transitions for SB **4** (Figure 4). See ref 22 and Petke et al. (Petke, J. D.; Maggiora, G. M.; Shipman, L. L.; Christoffersen, R. E. *J. Mol. Spectrosc.* **1978**, *71*, 64–84) for porphyrin calculations.

(26) P. M. Callahan and G. T. Babcock, unpublished results.

(27) Although "Q_x" and "Q_y" for SBH$^+$ **1** are only 26.5° apart, these transitions conform to the four-orbital model. Q_y is coparallel with and is composed of the $b_1 \rightarrow c_1$ and $b_2 \rightarrow c_2$ promotions. Likewise, Q_x is coparallel with and is composed of the $b_1 \rightarrow c_2$ and $b_2 \rightarrow c_1$ promotions. There is essentially no cross mixing. This is not always the case for the Soret transitions.

(28) Sutherland, J. C.; Olson, J. M. *Photochem. Photobiol.* **1981**, *33*, 379–84.

Table II. Calculated Transition Dipole Moment Orientations

	Schiff base			protonated Schiff base			$\theta_{SB} - \theta_{SBH^+}$,
compd	transition,[a,b] nm	θ,[c] deg	$\theta_y - \theta_x$, deg	transition,[a,b] nm	θ,[c] deg	$\theta_y - \theta_x$, deg	deg
1	Q_y 644	21.2	88.8	Q_y 700	7.6	26.5	13.6
	Q_x 631	−67.6		Q_x 656	−18.9		−48.7
	B_y 359	11.9	66.8	Soret 1 490	−6.8		
	345	70.1		466	−47.6		
	B_x 343	−54.9		454	−56.0		
				Soret 2 346	19.9		
				335	−62.2		
				324	−30.7		
3	Q_y 651	15.05	88.1	Q_y 766	13.3	67.4	1.75
	Q_x 630	−73.05		Q_x 655	−45.1		−18.95
	B_y 359	16.7	81.6	Soret 1 416	−47.0		
	B_x 347	−64.9		Soret 2 342	29.9		
				309	35.5		
				288	80.7		
4	Q_y 690	15.2	78.4	Q_y 788	65.6	66.6	−50.3
	Q_x 583	−86.4		Q_x 645	−1.1		−85.3
	x 374	77.2		Soret 1 485	−77.9		
	x 366	−71.0		457	−33.7		
	y 338	−7.1		Soret 2 347	60.2		
	y 332	−0.7		344	69.5		
				327	−20.9		
5	Q_y 804	16.7	72.1	Q_y 889	54.0	83.7	−37.3
	Q_x 611	88.8		Q_x 672	−42.3		−48.9
	385	89.5		Soret 1 461.5	−79.0		
	332	−52.8		399.5	−35.7		
	310	9.0		Soret 2 327	52.3		
	301	44.9		320	62.0		
				294	−35.7		
				281	3.3		
pyrochl	Q_y 662	−6.6	24.6	Q_y 603	11.5	31.6	−18.1
ketimine	Q_x 534	18.0		Q_x 494	−20.1		38.1
	B_x 369	−75.3	89.0	380.5	−48.4		
	B_y 343	15.7		327	40.9		
				319	−39.0		
pyrochl	Q_y 727	−0.4	13.1	Q_y 683	3.9	17.5	−4.3
enamine	Q_x 547	12.7		Q_x 496	−13.6		26.3
	467	−40.3		378	−43.1		
	397	−26.4		321	30.6		
	382	−31.2					
	370	−71.5					
	347	−46.3					

[a] Only the more intense Soret transitions are given. [b] The labels Q_y, Q_x, B_y, and B_x have been assigned on the basis of the one-electron promotions which give rise to the transition $(b_1 \rightarrow c_1) \pm (b_2 \rightarrow c_2)$ for B_y, Q_y and $(b_1 \rightarrow c_2) \pm (b_2 \rightarrow c_1)$ for B_x, Q_x (see Figure 6). The Soret region of SB **4** consists of four intense transitions (Figure 4). None of these transitions is composed primarily of the one-electron promotions predicted by the four-orbital model. Thus they have been labeled either "*x*" or "*y*" to indicate their polarization, but not B_x or B_y. [c] θ lies in the *xy* plane, the plane of the macrocycle; $\theta = 0°$ along the *y* axis. For the porphyrins **1** and **3**, *y* is defined by the pyrrole nitrogens of the vinyl- and SB-substituted rings. For **4**, **5**, and the PChl derivatives, *y* is defined by the pyrrole nitrogens of the unsaturated rings (rings I and III of PChl). $\theta > 0$ indicates a counterclockwise rotation relative to 0°. All angles are presented so that θ, $\Delta\theta < 90°$

proximately 90° apart. Although for the SBH^+ **4** and **5** derivatives individual transition dipoles are predicted to rotate by as much as 85°, the changes in the relative orientations of Q_y to Q_x are not appreciable. This result is intriguing because it has been suggested[30] that the bacteriochlorophyll *a* (BChl) in the red-shifted, 800 nm absorbing BChl *a*-protein from the green photosynthetic organism *Prosthecochloris aestuarii* strain 2K have their Q_y transitions rotated by 90° relative to monomeric BChl *a* in solution. MCD spectroscopy, which is sensitive only to the *relative*, not absolute, orientations of the transition dipoles, showed[28] that the protein did not differ from monomeric BChl *a* in solution. Thus either no rotation of Q_y has taken place or both Q_y and Q_x rotate. Our theoretical results on similar chromophores demonstrate that a perturbation may induce rotations of both Q_y and Q_x.[31,32]

Chlorin Resonance Raman. Figure 8 shows the high frequency region (1100–1800 cm^{-1}) resonance Raman spectra of the al-

(29) The Q_y transition dipole moment direction for a C- or BC-type macrocycle has been determined for ZnPChl *a* and was found to be perpendicular to the axis containing the reduced ring, as we and many others have predicted. (Kuki, A.; Boxer, S. G. *Biochemistry* **1983**, *22*, 2923–33).

(30) Pearlstein, R. M.; Hemenger, R. P. *Proc. Natl. Acad. Sci. U.S.A.* **1978**, *75*, 4920–4.

(31) The protonation of the Schiff base derivatives of PChl *a* also results in small changes of Q_x relative to Q_y. In contrast to SBH^+ **4** and **5**, the axes do not rotate much. The predicted angle between Q_x and Q_y is very small for both the ketimine and enamine SB and SBH^+ derivatives (Table II). Although the Q_x in these systems is composed primarily of the $b_1 \rightarrow c_2$ and $b_2 \rightarrow c_1$ (*x*-polarized) promotions, they essentially cancel, resulting in the *net* dipole being dominated by a small $b_1 \rightarrow c_1$ (*y*-polarized) contribution. The Q_x calculated for Chl *a* by the ab initio molecular fragment technique (Petke, J. D.; Maggiora, G. M.; Shipman, L. L.; Christoffersen, R. E. *Photochem. Photobiol.* **1979**, *30*, 203–23) is also more "*y*" than "*x*". In this case, the Q_x is more complex and is comprised of many configurations with dipoles of approximately equal but small magnitude which are oriented in many different directions.

(32) The calculations not only reproduce the effects of protonation of the Schiff base substituents but also correctly predict another facet tangential to the main point of this paper: low-lying Ni(II) d → d transitions (below the $\pi \rightarrow \pi^*$). The singlets lie in the near IR and the triplets at even lower energies. On the basis of extended Hückel calculations, Ake and Gouterman suggested that Ni porphyrins are nonluminescent because of quenching by these transitions (Ake, R. L.; Gouterman, M. *Theor. Chim. Acta* **1970**, *17*, 408–16). Direct evidence for short-lived $^{3,1}(d_{z^2},d_{x^2-y^2})$ states has been obtained from picosecond spectroscopy (Kim, D.; Kirmaier, C.; Holton, D. *Chem. Phys.* **1983**, *75*, 305–22).

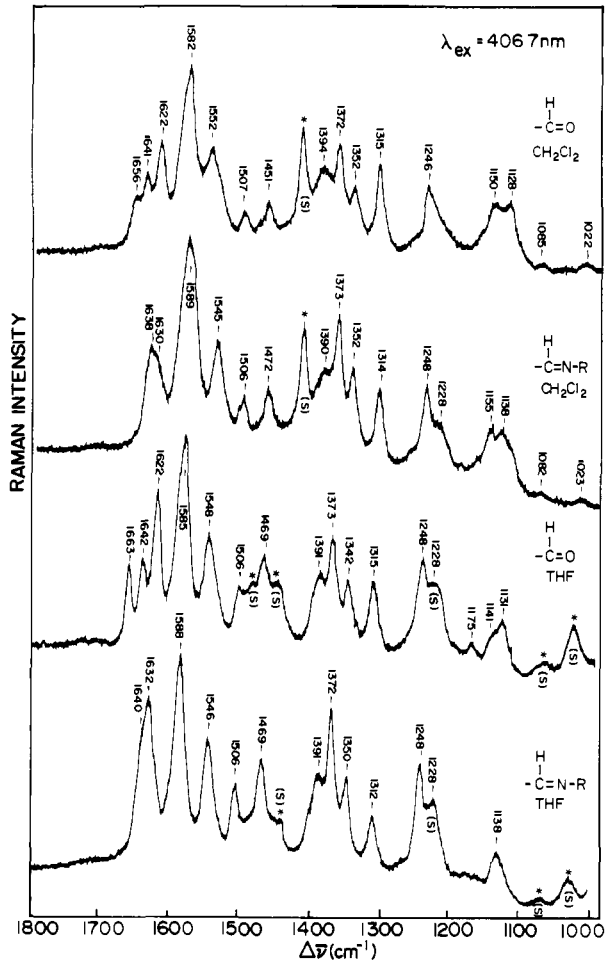

Figure 8. Soret region resonance Raman spectra of the aldehyde and Schiff base chlorins **4b** and **4c** in CH_2Cl_2 and THF with 406.7-nm laser excitation. Vibrational modes due to the solvent are marked by an asterisk.

dehyde and Schiff base adducts of Cu chlorin, **4b**, and **4c**,[12] in CH_2Cl_2 and THF with 406.7-nm (Soret) excitation. The low frequency (0–1000 cm^{-1}) region spectra were masked by solvent vibrations and are not reproduced here. Although one ring of this copper tetrapyrrole compound is reduced, its Soret region resonance Raman spectrum displays vibrations typical of the more symmetric copper porphyrin molecules.[10,26] However, the number of bands observed is increased owing to the lowered symmetry of the chlorin.[23] These bands correspond to the A_{1g}, A_{2g}, B_{1g}, and B_{2g} symmetry vibrations in D_{4h} nomenclature. The intensities of all the vibrations are approximately equal in contrast to metalloporphyrin spectra where the A_{1g} modes dominate.

From the optical spectra and titration behavior of the aldehyde,[11] it has been deduced that an intramolecular hydrogen bond forms between the C=O and an adjacent hydroxyl substituent in CH_2Cl_2 but not in THF. (In THF, the OH group interacts predominantly with solvent molecules.) These observations are supported by the resonance Raman spectra. The highest frequency vibrations of the aldehyde **4b** in CH_2Cl_2 and THF occur at 1656 and 1663 cm^{-1}, respectively. These are assigned to the ν_{CO} stretching frequencies by analogy with formyl-substituted metalloporphyrins.[34] The 7-cm^{-1} variation in $\nu_{CH=O}$ between CH_2Cl_2 and THF represents a hydrogen bond strength of approximately 1 kcal/mol, which predicts an optical red shift of 93 cm^{-1}.[34a] This is in qualitative agreement with the observed shift of 169 cm^{-1}.

The resonance Raman spectra of the aldehyde show that the π electron density sensitive marker band at 1373 cm^{-1} (ν_4, A_{1g}) and core-size marker bands at 1641 cm^{-1} (ν_{10}, B_{1g}), 1582 cm^{-1} (ν_2, A_{1g}; ν_{19}, A_{2g}), and 1507 cm^{-1} (ν_3, A_{1g}) are not affected by hydrogen bonding at the ring periphery. Vibrations that are affected are the following: (i) 1552 (CH_2Cl_2) to 1548 cm^{-1} (THF), (ii) 1451 (CH_2Cl_2) to 1469 cm^{-1} (THF), (iii) 1352 (CH_2Cl_2) to 1342 cm^{-1} (THF), and (iv) 1150 (CH_2Cl_2) to 1141 cm^{-1} (THF). These vibrations may involve C_β–C_β, C_β–C_{subst} stretching or CHO bending character;[35] however, further analysis is not possible at the present time. The mode observed at 1622 cm^{-1} is assigned to the C=C stretch of the acroleinyl substituent by analogy with similar group frequencies.[36]

Formation of the Schiff base does not affect the chlorin ring vibrations (Figure 8): below 1600 cm^{-1} the band positions and profiles of the aldehyde and SB are nearly identical for a given solvent. The major changes upon Schiff base formation[37] are the disappearance of the acroleinyl C=O and C=C stretching frequencies at ~1660 and 1622 cm^{-1}, respectively, and the appearance of a band at ~1630 cm^{-1}. This new vibration is assigned to the C=NR vibration by analogy to previously reported assignments.[10] Due to overlap with a band at approximately 1640 cm^{-1} the exact position of the C=NR vibration cannot be determined. Both resonance Raman and optical data suggest that the Schiff base also forms an intramolecular hydrogen bond in CH_2Cl_2. In the absorption spectrum this is reflected as a 225-cm^{-1} red shift of the visible band and an overlapped splitting of the Soret.[11] From the resonance Raman, comparison of the 1640–1630-cm^{-1} region of SB **4c** in CH_2Cl_2 and THF reveals that in THF the overlapping bands are more intense and narrower than those in CH_2Cl_2. We interpret this as an increase of $\nu_{C=N}$ due to an intramolecular hydrogen bond to the 7-OH group in CH_2Cl_2. Other evidence is obtained from the 1150–1130-cm^{-1} region. For CHO and CHNR there are two bands in CH_2Cl_2 (CHO: 1150, 1128 cm^{-1}; CHNR: 1155, 1138 cm^{-1}), while in THF these bands apparently collapse (CHO: 1141, 1131; CHNR: 1138 cm^{-1}). Other bands which were solvent sensitive for the aldehyde **4b** are not affected. Neither are the chlorin ring vibrations.

These results on the aldehyde and Schiff base derivatives of the chlorin demonstrate that effects of the CHO and CHNR groups are localized, not delocalized into the π system of the chlorin, in excellent agreement with the calculations.

Figure 9 presents the high frequency (1000–1800 cm^{-1}) resonance Raman spectra of the protonated Schiff base **4c·HCl** in CH_2Cl_2 and THF and the pyrrolidinium adduct[38] **4d·ClO$_4^-$** in THF with 406.7- and 488.0-nm laser excitation. These two excitation frequencies correspond approximately to the Soret maxima of **4c·HCl** and **4d·ClO$_4^-$**. Excitation at 488.0 nm of the SBH^+ **4** produces resonance Raman spectra which display a peripheral C=$^+$NHR stretching vibration of 1646 cm^{-1} in CH_2Cl_2 and 1650 cm^{-1} in THF. These values are typical for $\nu_{C=N}$ of protonated Schiff bases[11] and have been observed in IR spectra as well. This vibration is absent in the spectra resulting from 406.7-nm excitation. Further comparison of the resonance Raman spectra of SBH^+ with 406.7- and 488.0-nm excitation reveals large intensity differences between the two spectra. With 488.0-nm excitation, the totally symmetric A_{1g} modes at 1592, 1502, and 1375 cm^{-1} are decreased in intensity relative to the nontotally symmetric vibrations. This pattern was also observed for SB **1c·HCl**.[10] The frequencies of the SBH^+ **4** and SB **4** vibrations are similar. Again, as found for **1**, protonation does not greatly perturb the macrocycle π bonding in the ground state.

(33) Ozaki, Y.; Kitagawa, T.; Ogoshi, H. *Inorg. Chem.* **1979**, *18*, 1772–6.
(34) (a) Babcock, G. T.; Callahan, P. M. *Biochemistry* **1983**, *22*, 2314–19. (b) Van Steelandt-Frentrup, J.; Salmeen, I.; Babcock, G. T. *J. Am. Chem. Soc.* **1981**, *103*, 5981–2. (c) $\nu_{C=O}$ for α_s-methylcinnamaldehyde occurs at 1658 cm^{-1} ($CHCl_3$). Dolphin, D.; Wick, A. "Tabulation of Infrared Spectral Data"; Wiley-Interscience: New York, 1977, p 37.

(35) (a) Abe, M.; Kitagawa, T.; Kyogoku, Y. *J. Chem. Phys.* **1978**, *69*, 4526–34. (b) Choi, S.; Lee, J. J.; Wei, Y. H.; Spiro, T. G. *J. Am. Chem. Soc.* **1983**, *105*, 3692–707. (c) Green, J. H. S.; Harrison, D. J. *Spectrochim. Acta, Part A* **1976**, *32A*, 1265–77.
(36) $\nu_{C=C}$ of α,β-unsaturated aldehydes ranges from 1618 to 1695 cm^{-1} (ref 34c, p 170).
(37) By analogy, $\nu_{C=O}$ and $\nu_{C=C}$ occur at 1674 and 1622 cm^{-1}, respectively, for cinnamaldehyde. Monitoring *n*-butyl Schiff base formation of cinnamaldehyde by IR absorption in CH_2Cl_2 resulted in the disappearance of ν_{CHO} and $\nu_{C=C}$ with the concomitant appearance of a band at 1632 cm^{-1} (C=N) and a very weak band at 1614 cm^{-1} (C=C). (B. Ward, unpublished results).

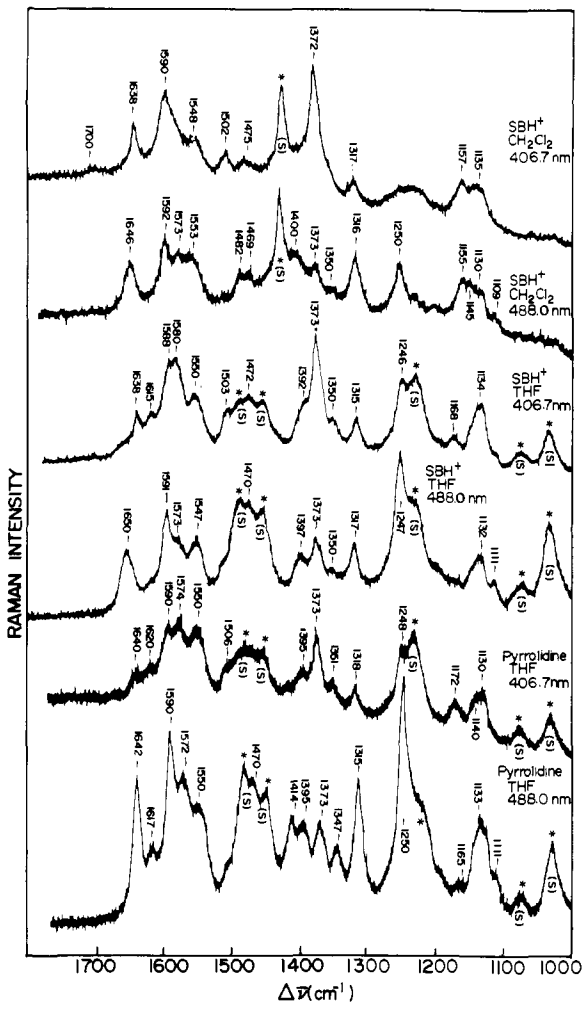

Figure 9. Resonance Raman spectra with 406.7- and 488.0-nm laser excitation of the protonated Schiff base **4c·HCl** (in CH_2Cl_2 and THF) and the pyrrolidinium perchlorate adduct **4d·ClO$_4^-$** in THF.

The absent or extremely weak peripheral C=N vibration with excitation at 406.7 nm and its presence with 488.0-nm excitation, as well as the less intense totally symmetric vibrations with excitation at 488.0 nm relative to 406.7 nm, also occur for the pyrrolidinium adduct. $\nu_{C=N}$ is 1642 cm^{-1} in THF, a typical value for aromatic iminium salts.[39]

These spectra clearly demonstrate selective enhancement of the peripheral C=N vibration, which occurs only with excitation into the lower-energy branch of the Soret. The enhancement remains constant from 488 nm down to ~440 nm, below which a rapid fall off occurs (data not shown). The region from the Soret maximum down to 440 nm includes fundamental (0–0) and vibronic (0–1) bands, both of which should contribute to the resonance enhancement of the same vibrations, according to theory.[40] The INDO-CI calculations on SBH$^+$ **4** place two transitions under the lower-energy Soret, both of which contain SB C=N π^* character. Thus excitation of these transitions (and their overtones) should lead to resonance enhancement of $\nu_{C=N}$, as observed. Similarly, the transitions comprising the higher-energy branch of the Soret contain little SB C=N π^* character in excellent agreement with the absence of $\nu_{C=N}$ in the resonance Raman spectra with 406.7-nm excitation.[41]

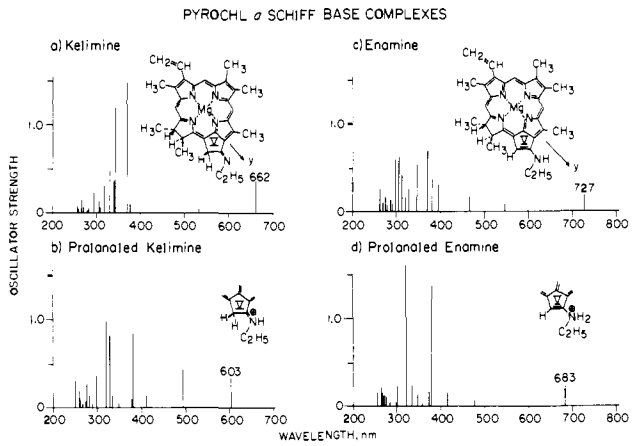

Figure 10. Calculated spectra (oscillator strength vs. λ) of the unprotonated and protonated ketimine (a, b) and enamine (c, d) isomers of pyrochlorophyllide *a* Schiff base derivatives.

Pyrochlorophyll *a* Schiff Base Derivatives. Recent suggestions for the red-shifted donor Chls in green plant reaction centers have included the derivatization of the ring V carbonyl to a Schiff base by an amine side chain of the protein.[8,9] Red shifts of 23 and 26 nm have been reported for Schiff base complexes of methyl pyrochlorophyllide *a*[8] and nickel pyrochlorophyll *a*,[9] respectively, upon exposure to acidic media. Both the SB and SBH$^+$ derivatives have been assigned to the ketimine form (see Figure 10) on the basis of IR and NMR data.[9]

The calculated spectra of the two possible isomeric Schiff base forms for PChl, ketimine and enamine, are shown in Figure 10. They predict a blue shift of the Q_y band of either isomer upon protonation and that the enamine should absorb to the red of the ketimine.[42] The calculated shifts upon protonation are 662 → 603 nm for the ketimine and 727 → 683 nm for the enamine. These results are obtained for Ni as well as Mg complexes.

As a test of the self-consistency of the calculations, models were examined which were modified either by cleavage of ring V or by oxidation of the reduced ring IV. Blue shifts are also calculated for chlorins where ring V has been cleaved, i.e., 2-vinyl-6-SB-substituted chlorins which are saturated at positions 7 and 8, whereas protonation of a Ni pheoporphyrin Schiff base (the porphyrin analogue of PChl and equivalent to SB **1** with a fifth ring) results in a red shift. The shift behavior of the Q_y band of a chlorin Schiff base complex thus depends on the position of the Schiff base substituent relative to the saturated ring and is not influenced by the presence or absence of ring V. Chlorin SB **4**, which red shifts upon protonation, is a b-type chlorin with the Schiff base substituted directly onto the ethylidine group of the saturated ring. The Schiff base substituents of the PChl sit on the ring adjacent to the saturated ring.

The calculations predict that the only way to obtain a net red shift upon protonation of a SB-PChl is by isomerization of the ketimine to the enamine. A red shift of 21 nm from ketimine to protonated enamine is calculated, in agreement with observed values. This represents a minimum shift since the calculations

(38) The chlorin pyrrolidine adduct, **4d·ClO$_4$** (see preceding paper), has an optical spectrum similar to that of the protonated Schiff base species: split Soret band with maxima at 403 and 494 nm and a red-shifted visible band at 744 nm in THF.

(39) Leonard, N. J.; Paukstelis, J. V. *J. Chem. Soc.* **1963**, *28*, 3021–4.

(40) Felton, R. H.; Yu, N.-T. In "The Porphyrins"; Dolphin, D., Ed.; Academic Press: New York, 1978, Vol. 3, pp 347–99.

(41) Since resonance Raman enhancement depends on a shift in the equilibrium bond length between the ground and excited states, we assume that excitations into excited states which contain essentially no C=N character will not result in a change in the C=N bond length and that C=N enhancement will not occur. Conversely, excitation into excited states with appreciable C=N antibonding π^* character should result in a lengthening of the C=N bond and enhancement of the $\nu_{C=N}$.

(42) Enol derivatives of Chl *a* absorb to the red of the keto form. The red absorption band at 750–800 nm is very weak (Wasielewski, M. R.; Thompson, J. F. *Tetrahedron Lett.* **1978**, 1043–6. Hynninen, P. H.; Wasielewski, M. R.; Katz, J. J. *Acta Chem. Scand., Ser. B* **1979**, *B33*, 637–48). This low-energy transition is predicted by charge iterative extended Hückel calculations (Hanson, L. K.; Newman, A. R.; Richardson, P. F.; Fajer, J. "Proceedings of the 5th DOE Solar Photochemistry Research Conference"; 1981, p 33) and molecular fragment ab initio calculations (Petke, J. D.; Shipman, L. L.; Maggiora, G. M.; Christoffersen, R. E. *J. Am. Chem. Soc.* **1981**, *103*, 4622–3).

were performed on bare charged species with no counterions present. Diffusion of the charge by solvation and/or ion pairing with counterions should result in larger red shifts because the uncharged enamine is predicted further to the red. The ketimine and protonated enamine have calculated spectra which are most like Chl *a* in contrast to the protonated ketimine, which has an additional intense transition at 494 nm.

The ground-state energies of both isomers drop with protonation, the enamine somewhat less than the ketimine. As with species **1-5**, protonation should render PChl (and Chl) Schiff base derivatives more difficult to oxidize.

The protonated enamine PChl *a* predicted by the calculations apparently contradicts experimental evidence. Resonance Raman spectroscopy should provide another diagnostic tool for distinguishing between the two isomers. Not only should the C-N stretch differ substantially, but ring V also becomes an integral part of the macrocycle π system in the enamine.

Our resonance Raman results demonstrate the similarity between hydrogen-bonded C=O and protonated C=N vibrational stretching frequencies and the isolation of the peripheral C=O or C=N substituent from the macrocycle ground state. Thus, the resonance Raman spectra which have been interpreted as arising from hydrogen-bonded Chl *a* in in vivo preparations[43] could also be due, in part, to ketimine SB derivatives.[44]

The calculations predict that protonation affects the SB derivatives of PChl somewhat differently than the SB derivatives of **1-5**. Nonetheless, our results suggest that SBH^+ substituents on chlorophyll would enhance the ability of protein environments to modulate spectral and redox properties. Schiff base derivatives of chlorophyll pigments thus warrant further serious consideration as models for electron donors within photosynthetic reaction centers.

Acknowledgment. We thank Michael Zerner for his INDO program, R. M. Pearlstein and G. M. Maggiora for results prior to publication, and G. M. Maggiora and J. Fajer for helpful comments and discussions. This work was supported by the Division of Chemical Sciences, U.S. Department of Energy, under Contract No. DE-AC02-76CH00016 at Brookhaven National Laboratory and by NIH (GM25480 to GTB) and NSF (CKC) at Michigan State University. C.K.C. is an Alfred P. Sloan Fellow (1980-1984) and a Camille and Henry Dreyfus Teacher-Scholar (1981-1985).

Registry No. CHO **1b**, 84195-13-1; SB **1c**, 84195-14-2; SBH^+ **1c**·ClO_2^-, 90432-99-8; diCHO **2b**, 90413-26-6; diSB **2c**, 90413-27-7; SB,SBH^+ **2c**·ClO_4^-, 90433-00-4; diSBH^+ **2c**·$(ClO_4^-)_2$, 90433-01-5; diCHO **3b**, 90413-28-8; diSB **3c**, 90413-29-9; SB,SBH^+ **3c**·ClO_4^-, 90433-02-6; diSBH^+ **3c**·$(ClO_4^-)_2$, 90433-03-7; CHO **4b**, 90413-30-2; SB **4c**, 90413-31-3; SBH^+ **4c**·ClO_4^-, 90413-47-1; diCHO **5b**, 90413-35-7; diSB **5c**, 90413-36-8; diSBH^+ **5c**·$CF_3CO_2^-$, 90433-05-9.

(43) (a) Lutz, M. *J. Raman Spectrosc.* **1974**, *2*, 497-516. (b) Lutz, M.; Brown, J. S.; Remy, R. In "Chlorophyll Organization and Electron Transfer in Photosynthesis"; Elsevier: Amsterdam, 1979; Ciba Foundation Symposium 61, pp 105-25.

(44) PS I and PS II reaction centers which are free of antenna pigment have not yet been isolated.

Kinetic Applications of Electron Paramagnetic Resonance Spectroscopy. 42. Some Reactions of the Bis(trifluoromethyl)aminoxyl Radical[1]

T. Doba[2] and K. U. Ingold*

Contribution from the Division of Chemistry, National Research Council of Canada, Ottawa, Ontario, Canada K1A 0R6. *Received October 12, 1983. Revised Manuscript Received January 27, 1984*

Abstract: Absolute rate constants have been determined in Freon solvents over a temperature range from ca. 190 to 300 K for H atom abstraction by $(CF_3)_2NO\cdot$ from 11 substrates and for the addition of this radical to $CH_2{=}CCl_2$. Some values found for log A (M^{-1} s^{-1}) and E_a (in kcal/mol) are 5.8 ± 0.6 and 10.7 ± 0.7 for cyclopentane, 6.5 ± 0.3 and 5.7 ± 0.5 for 1,4-cyclohexadiene, 5.3 ± 0.3 and 6.9 ± 0.3 for benzaldehyde, 4.8 ± 0.2 and 3.3 ± 0.3 for 2,4,6-tri-*tert*-butylphenol, 5.9 ± 0.7 and 4.3 ± 0.7 for tri-*n*-butylstannane, and 5.3 ± 0.4 and 9.3 ± 0.5 for $CH_2{=}CCl_2$. The preexponential factors are uniformly smaller than the values generally considered "normal" for radical/H atom abstractions and radical/C=C double-bond additions, viz., $10^{8.5\pm0.5}$ M^{-1} s^{-1}. It is concluded that the low A factors are not due to tunneling. It is suggested that they are probably due to geometric constraints on the transition states. For a wide range of substrates exhibiting very different reactivities the absolute rate constant for H atom abstraction by $(CF_3)_2NO\cdot$ and by $Me_3COO\cdot$ at ambient temperatures are virtually equal.

Bis(trifluoromethyl)aminoxyl, $(CF_3)_2NO\cdot$, which was first reported in 1965,[3,4] is a remarkable free radical. It is both more persistent[5] and more reactive than the better known di-*tert*-alkylaminoxyl radicals.[6] There have been some studies of its physical properties[7,8] and numerous studies of the products formed when $(CF_3)_2NO\cdot$ reacts with organic compounds: hydrogen atom abstractions, additions to multiple bonds, and substitution processes having been identified.[9] However, the only kinetic data available

(1) Issued as NRCC No. 23403. Part 41: Anpo, M.; Sutcliffe, R.; Ingold, K. U. *J. Am. Chem. Soc.* **1983**, *105*, 3580-3583.

(2) NRCC Research Associate 1982-1984.

(3) Blackley, W. D.; Reinhard, R. R. *J. Am. Chem. Soc.* **1965**, *87*, 802-805.

(4) Makarov, S. P.; Yakubovich, A. Ya.; Dobov, S. S.; Medvedev, A. N.; *Dokl. Akad. Nauk SSSR* **1965**, *160*, 1319-1322.

(5) It does not undergo thermal decomposition even at 200 °C; see: Makarov, S. P.; Englin, M. A.; Videiko, A. F.; Tobolin, V. A.; Dobov, S. S. *Dokl. Akad. Nauk SSSR* **1966**, *168*, 344-347.

(6) For review of the chemistry of $(CF_3)_2NO\cdot$, see: (a) Babb, D. P.; Shreeve, J. N. *Intra-Sci. Chem. Rep.* **1971**, *5*, 55-67. (b) Spaziante, P. M. *MTP Int. Rev. Sci.: Inorg. Chem., Ser. One* **1972**, *3*, 141-180. (c) Banks, R. E.; Barlow, M. G. *Fluorocarbon Relat. Chem.* **1971**, *1*, 109-115. (d) Banks, R. E. *Ibid.* **1974**, *2*, 223-235.

(7) Chatgilialoglu, C.; Malatesta, V.; Ingold, K. U. *J. Phys. Chem.* **1980**, *84*, 3597-3599.

(8) Compton, D. A. C.; Chatgilialoglu, C.; Mantsch, H. H.; Ingold, K. U. *J. Phys. Chem.* **1981**, *85*, 3093-3100.

(9) For leading references, see ref 10.

0002-7863/84/1506-3958$01.50/0 Published 1984 by the American Chemical Society